Control of the spatiotemporal emission of a broad-area semiconductor laser by spatially filtered feedback

Shyam K. Mandre, Ingo Fischer, and Wolfgang Elsässer

Institute of Applied Physics, Darmstadt University of Technology, Schlossgartenstrasse 7, D-64289 Darmstadt, Germany

Received December 13, 2002

We demonstrate the control of the spatiotemporal emission dynamics of a broad-area semiconductor laser in an external optical feedback configuration formed by a spatially filtering mirror. The emission properties are studied with a single-shot streak camera with temporal resolution of ~7 ps and spatial resolution of ~5 μm. Our results show a significant reduction of the spatial filamentation and, furthermore, suppression of the spatiotemporal instabilities, which are both intrinsic emission properties of standard high-power broad-area lasers. Associated with the control of the emission dynamics, strong improvement of the beam quality, which is essential for numerous high-power applications, is possible. © 2003 Optical Society of America

OCIS codes: 140.5960, 190.3100, 140.3300, 190.4420.

Because of their wide emitting apertures, typically 50–200 μm, high-power semiconductor lasers, and in particular broad-area semiconductor lasers (BALs) exhibit the effects of beam filamentation[1,2] and spatiotemporal instabilities[3–7] originating from the nonlinear interaction of the intense optical field with the semiconductor medium. These spatiotemporal emission characteristics, resulting in a broad spectral bandwidth and a wide double-lobed far-field intensity profile, form a profound hindrance to the applicability of BALs as high-power laser devices in many conceivable fields, e.g., spectroscopy, material processing, and medicine. Therefore, control of the emission properties is vital for high-power applications. Besides these more technologically oriented aspects, control of the filamentation and dynamics is of significant physical interest,[8] as are the nonlinearities involved in the emission properties and the resulting spatiotemporal dynamics.[9]

Control of the emission properties of BALs can be pursued by different approaches. So far, several schemes to control the emission properties of BALs have been proposed and partly realized. One strategy has been to control the spectral emission properties. For high-power multistripe laser diodes, wavelength-selective components such as gratings[10] in external cavities have been used to narrow the broad spectral width. This control scheme can also be applied to BALs. Application of etalons[11] in external cavities has similarly resulted in narrowing the broad spectral width of BALs. Other strategies concentrate on narrowing the far-field intensity profile. Single narrow far-field lobe emission has been achieved by injection locking of a BAL in a master–slave-laser configuration[12] and by beam shaping in an external resonator configuration.[13] Other schemes involving spatially filtering feedback configurations to control the emission properties of BALs have been proposed.[14–16] A scheme applying curved mirrors as spatially filtering components has resulted in reduction of the static far-field beam divergence angle.[17] However, to our knowledge no experimental information about the underlying dynamic emission properties has been obtained so far.

In this Letter we present results of the comparison of the picosecond time-resolved spatiotemporal emission dynamics of a 100-μm-wide BAL in the solitary case, i.e., without optical feedback, and in an external cavity configuration with a spatially filtering component. With this configuration consisting of a lens and a plane mirror, we demonstrate substantial suppression of emission instabilities.

The BAL used for the measurements presented here is a commercial high-power InGaAsP device with 100-μm lateral stripe width operating at 807 nm. The front and rear facet reflectivities are 5% and 95%, respectively. This index-guided laser exhibits a threshold current of $I_{\mathrm{thr}} = 302$ mA and a nominal power of 1000 mW. To minimize thermal effects on the dynamics, we operated the BAL in pulse mode, with rectangular pulses of 30-ns length and a repetition rate of 100 Hz. A magnified image of the light-intensity distribution at the output facet is projected onto the input slit of a single-shot streak camera with temporal and spatial resolution of ~7 ps and ~5 μm, respectively. A common pulse generator serves as the trigger for the streak camera as well as the current source for the BAL. An adjustable delay line that is integrated within the setup allows selection of the temporal position of the spatiotemporal streak traces. A more detailed description of the detection setup can be found in Fischer *et al.*[6]

Before applying control to the BAL, we discuss its spatiotemporal emission dynamics under solitary operation at a pump current of $I_{\mathrm{pump}} = 1.75 I_{\mathrm{thr}}$, as displayed in Fig. 1. The horizontal and the vertical axis depict the intensity distribution across the active layer and its time evolution, respectively. Intensities are encoded in gray scales, with white representing maximum intensity. Figure 1(a) shows the turn-on dynamics of the BAL in a 4.4-ns-long time window, starting with the well-known relaxation oscillation peak, which is almost homogeneous across the lateral dimension. The transient relaxation oscillations are damped on a time scale of approximately 1000 ps. Already with the second relaxation oscillation peak the intensity distribution breaks up into multiple static filaments. In addition, on a time scale of 100–300 ps,

0146-9592/03/131135-03$15.00/0

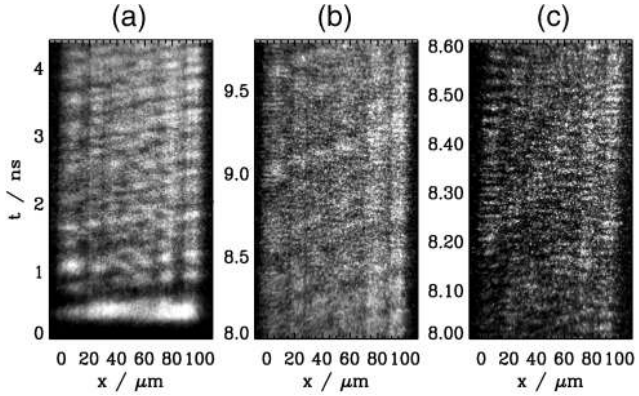

Fig. 1. Spatiotemporal emission dynamics of the near field of the solitary laser at $I_{\mathrm{pump}} = 1.75 I_{\mathrm{thr}}$: (a) Turn-on behavior in a 4.4-ns-long time window, (b) behavior 8 ns after turn-on in a 1.8-ns-long time window, and (c) behavior in a 600-ps-long time window.

a spatiotemporal instability can be seen that manifests itself as a lateral motion of intensity pulses across the laser facet. This instability, which is known as dynamic filamentation,[18] is a persistent phenomenon that can be observed even at later times, as depicted in Fig. 1(b), which displays the emission dynamics in a 1.8-ns-long time window 8 ns after turn-on. Here, one can also observe that the intensity pulses perform a zigzag movement across the laser facet. For example, at $t \simeq 9.6$ ns an intensity pulse originating from the right-hand side of the intensity profile bounces off the left margin and migrates back to the right. The physical origin of the static and dynamic filamentation has been discussed elsewhere.[5,6] In the 600-ps time window of Fig. 1(c), in addition to the dynamic filamentation, a longitudinal instability in the form of fast spiking of the light emission is visible that exhibits a period of the internal cavity round-trip time amounting to 28 ps.

To control the emission dynamics of the solitary BAL, we employ an external cavity configuration that consists of a spatially filtering component. For this purpose we have modified the control scheme proposed by Simmendinger *et al.*[14] Our setup is depicted in Fig. 2. The external cavity is made up of a cylindrical lens acting as a fast axis collimator with a focal length of $f = 0.91$ mm and a semitransparent ($R = 50\%$) plane mirror positioned approximately 1 cm from the laser facet. The top view reveals the principle of the spatial filtering, which is accomplished by the intrinsic beam divergence. The lateral angular alignment of the mirror is of substantial importance, as it determines under which angle the reflected beam is coupled into the active layer of the BAL. The effect of the angular alignment is shown in Fig. 3. The BAL was pumped slightly below the solitary threshold current, i.e., at $I_{\mathrm{pump}} = 0.98 I_{\mathrm{thr}}$. Laser emission was then induced by optical feedback. Figures 3(a)–3(c) display from left to right the intensity profiles along the output facet of the BAL with decreasing angle of the reflected beam to the optical axis of the laser. For variation of this angle the mirror was gradually tilted around the y axis, as indicated by the curved arrows in Fig. 2. Figure 3 clearly shows that the number of intensity peaks decreases with decreasing angle of incidence. When the mirror is aligned perpendicularly to the optical axis of the laser, only paraxial parts of the laser beam that have a comparatively low divergence angle, thus corresponding to lower-order lateral modes, are reflected back into the active layer of the BAL. This selective reflection results in single, zero-order lateral mode selection indicated by a single peak in the near-field intensity profile [Fig. 3(c)]. Further rotation of the mirror results in two, three, or more peaks again. The semitransparency of the mirror allows imaging of the near field of the front facet through the mirror onto the input slit of the streak camera.

For the following measurements we maintained the alignment of the mirror such that, at an operation current of $I_{\mathrm{pump}} = 0.98 I_{\mathrm{thr}}$, only one intensity peak was obtained, thus indicating zero-order lateral mode excitation. Then, the pump current was increased to a value above threshold. Figures 4(a) and 4(b) display 4.4-ns-long time windows of the BAL under feedback at $I_{\mathrm{pump}} = 1.75 I_{\mathrm{thr}}$ and $I_{\mathrm{pump}} = 3 I_{\mathrm{thr}}$, respectively. The bottom row shows the turn-on behavior, while the top row depicts the emission behavior 8 ns after turn-on. As in the solitary case, the turn-on sequence in Fig. 4(a) consists of a relaxation oscillation peak, whereas, in contrast to the solitary case, the emission after the first peak is predominantly

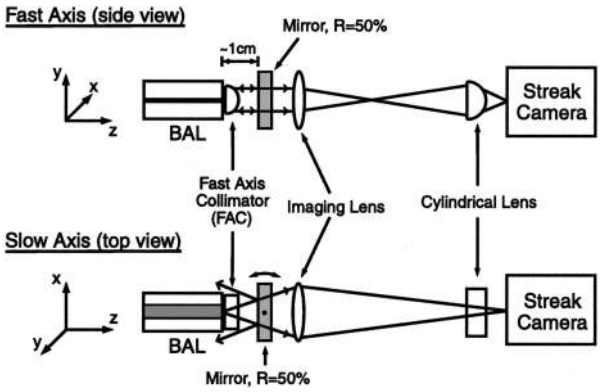

Fig. 2. Experimental setup of the external resonator configuration. Side view, active layer plane; top view, injection contact schematically indicated by the gray-shaded area.

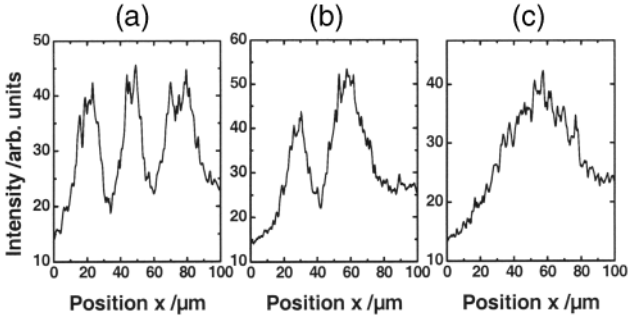

Fig. 3. Intensity profiles across the active layer of the BAL under feedback at $I_{\mathrm{pump}} = 0.98 I_{\mathrm{thr}}$. The angle of incidence on the mirror decreases from left to right.

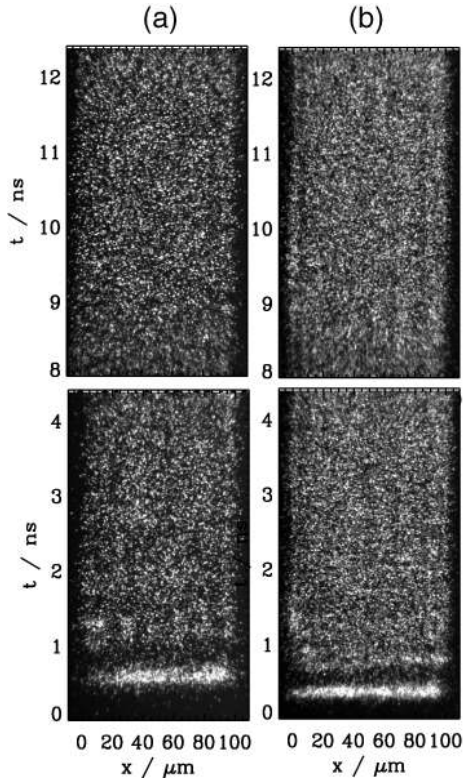

Fig. 4. Emission dynamics of the BAL subjected to spatially filtered optical feedback in 4.4-ns-long time windows. (a) $I_{\mathrm{pump}} = 1.75 I_{\mathrm{thr}}$ and (b) $I_{\mathrm{pump}} = 3 I_{\mathrm{thr}}$. Bottom row, turn-on behavior; top row, 8 ns after turn-on.

homogeneous across the laser facet and, even more, temporally stable. Even at a later time, 8 ns after turn-on, there is no considerable change visible in the emission behavior. In Fig. 4(b) a slight increase in the static filamentation is observable, in particular in the left marginal area of the laser. It seems that the control scheme described here has its limits concerning the static beam quality at those high pump rates. Thermal lensing may increasingly affect the beam characteristics at high pump currents, thus leading to degradation of the beam quality. Nevertheless, stabilization of the emission dynamics is still achieved by the scheme presented above even at high operation currents.

The spatiotemporal emission dynamics of the solitary BAL is associated with the broad spectral width and the multilateral and multilongitudinal emission of the BAL. Therefore, stabilization of the emission dynamics by spatially filtered feedback should lead to narrowing of the spectral width, or, more precisely, to the selection of a single, low-order lateral mode. Studies of the spectral or even spatiospectral emission properties of the BAL under feedback will also reveal the effect of spatially filtered optical feedback on the longitudinal mode behavior.

In conclusion, we have experimentally demonstrated stabilization of the emission dynamics of a conventional 100-μm-wide broad-area laser by spatially filtered optical feedback in an external cavity configuration. By lateral tilting of the mirror, single lateral modes can be selected, of which the zero-order mode seems to be most effective in stabilizing the emission. Altogether, the scheme promises the capability to control the emission properties of BALs.

This work was partly supported by the VW-Foundation and the Bundesministerium für Bildung und Forschung. S. K. Mandre's e-mail address is shyam.mandre@physik.tu-darmstadt.de.

References

1. G. H. B. Thompson, Opto-electronics **4,** 257 (1972).
2. R. J. Lang, A. G. Larsson, and J. G. Cody, IEEE J. Quantum Electron. **27,** 312 (1991).
3. N. Yu, R. K. DeFreez, D. J. Bossert, R. A. Elliott, H. G. Winful, and D. F. Welch, Electron. Lett. **24,** 1203 (1988).
4. H. Adachihara, O. Hess, E. Abraham, P. Ru, and J. V. Moloney, J. Opt. Soc. Am. **10,** 658 (1993).
5. O. Hess, S. W. Koch, and J. V. Moloney, IEEE J. Quantum Electron. **31,** 35 (1995).
6. I. Fischer, O. Hess, W. Elsässer, and E. Göbel, Europhys. Lett. **35,** 579 (1996).
7. T. Burkhard, M. O. Ziegler, I. Fischer, and W. Elsässer, Chaos Solitons Fractals **10,** 845 (1999).
8. J. V. Moloney, J. Opt. B Semiclass. Opt. **1,** 183 (1999).
9. J. R. Marciante and G. P. Agrawal, IEEE J. Quantum Electron. **32,** 590 (1996).
10. B. Chann, I. Nelson, and T. G. Walker, Opt. Lett. **25,** 1352 (2000).
11. W. Nagengast and K. Rith, Opt. Lett. **22,** 1250 (1997).
12. L. Goldberg and M. K. Chun, Appl. Phys. Lett. **53,** 1900 (1988).
13. V. Raab and R. Menzel, Opt. Lett. **27,** 167 (2002).
14. Chr. Simmendinger, D. Preisser, and O. Hess, Opt. Express **5,** 48 (1999), http://www.opticsexpress.org.
15. M. E. Bleich, D. Hochheiser, J. V. Moloney, and J. E. S. Socolar, Phys. Rev. E **55,** 2119 (1997).
16. R. Hochheiser, J. V. Moloney, and J. Lega, Phys. Rev. A **55,** R4011 (1997).
17. S. Wolff and H. Fouckhardt, Opt. Express **7,** 222 (2000), http://www.opticsexpress.org.
18. O. Hess, Proc. SPIE **2399,** 182 (1995).